Topological analysis of chaos in neural spike train bursts

R. Gilmore
Department of Physics and Atmospheric Science, Drexel University, Philadelphia, Pennsylvania 19104

Xing Pei and Frank Moss
Center for Neurodynamics, University of Missouri, St. Louis, Missouri 63121

(Received 4 February 1999; accepted for publication 10 May 1999)

We show how a topological model which describes the stretching and squeezing mechanisms responsible for creating chaotic behavior can be extracted from the neural spike train data. The mechanism we have identified is the same one (''gateau roulé,'' or jelly-roll) which has previously been identified in the Duffing oscillator [Gilmore and McCallum, Phys. Rev. E **51**, 935 (1995)] and in a YAG laser [Boulant *et al.*, Phys. Rev. E **55**, 5082 (1997)]. © *1999 American Institute of Physics.* [S1054-1500(99)01903-5]

A class of temperature sensitive neurons contain oscillators or pacemakers. These neurons show bifurcations among several regular firing patterns that can be selected using temperature as the control parameter. Examples include the multimodal electroreceptors of the dogfish, catfish, and paddlefish, the warm and cold receptors of the rat and cat and hypothalamic neurons in rat brain. For certain conditions, these neurons show bursts from two to several closely spaced action potentials followed by longer silences. Indeed, bursting is one of the most commonly observed neural responses. Bursting and regular (together with several other) firing patterns can be mimicked by a simple Hodgkin–Huxley model modified by the addition of a pair of slow Na^+ and K^+ conductances. We show that all bursting patterns observed arise directly from the topology of the underlying chaotic attractor characteristic of this model and that this attractor falls within the same topological class as the previously analyzed YAG laser. Thus, familiar burst patterns observed experimentally in a large class of neurons result from chaotic attractors of a single classifiable topology.

I. INTRODUCTION

In a beautiful series of experiments more than 40 years ago, Hodgkin, Huxley, and Katz determined a mechanism responsible for the propagation of electric pulses along the axon of a giant squid nerve cell.[1] Hodgkin and Huxley also proposed a simple model to describe the time evolution and the propagation of these electrical pulses.[2] This model, and variations on it, have been used to describe propagation of nerve action potentials ever since.

Hodgkin and Huxley determined that changes in the potential difference across the axon membrane are due principally to the flow of ions through the membrane and along the axis of the nerve cell axon. The ionic species which contribute most substantially to the current flows are Na^+, K^+, and Cl^-. The cell membrane itself acts like a capacitor with capacitance C_M. Under rest conditions, the membrane is polarized, so that the interior potential is less than the exterior potential by about 65 mV ($V_{\text{interior}} - V_{\text{exterior}} \simeq -65$ mV). This potential difference is maintained by ion pumps. Under rest conditions, the three species exhibit concentration gradients across the cell membrane. The concentration of K^+ ions within the axon is larger than the concentration outside by a large factor ($[K^+]_{\text{inside}}/[K^+]_{\text{outside}} \simeq 20$), while the reverse is true for Na^+ and Cl^-:$[Na^+]_{\text{inside}}/[Na^+]_{\text{outside}} \simeq 1/9$; $[Cl^-]_{\text{inside}}/[Cl^-]_{\text{outside}} \simeq 1/6$. These ratios depend on the potential difference, V, and weakly on the temperature, T.

At rest, the membrane is negatively polarized. As the sodium channel opens, a relatively fast influx of Na^+ ions takes place, and the membrane becomes depolarized (V increases and subsequently becomes positive). After a short time ($\sim$1 ms) this influx turns off and a fast efflux of K^+ begins. While this takes place there is also a slow efflux of Na^+ as the Na^+ concentration gradient is restored. The fast K^+ efflux is also followed by a slower K^+ influx to restore the K^+ concentration gradient. All flows in the Na^+ cycle (fast influx, slow efflux) and K^+ cycle (fast efflux, slow influx) occur with different time scales.

Hodgkin and Huxley proposed the following equation to describe the current flow, I, into a Gaussian pillbox whose walls consist of the axon membrane bounded by two circular sections perpendicular to the axis,

$$I = C_M \frac{dV}{dt} + I_{Na^+} + I_{K^+} + I_{Cl^-}. \tag{1}$$

Here C_M is the capacitance of the membrane and I_{Na^+}, I_{K^+}, and I_{Cl^-} are the ion current flows through the membrane. These current flows are proportional to the conductance and the differences between the potential (V) and the respective equilibrium potentials,

$$\begin{aligned} I_{Na^+} &= g_{Na^+}(V - \mu_{Na^+}), \\ I_{K^+} &= g_{K^+}(V - \mu_{K^+}), \\ I_{Cl^-} &= g_{Cl^-}(V - \mu_{Cl^-}). \end{aligned} \tag{2}$$

The Na^+ and K^+ conductances are sensitively dependent on the potential V. Hodgkin and Huxley proposed the following phenomenological expressions for these conductances:

$$g_{Na^+}=m^3h\bar{g}_{Na^+} \quad \frac{dm}{dt}=-(m-m_\infty)/\tau_1,$$
$$g_{K^+}=n^4\bar{g}_{K^+} \quad \frac{dh}{dt}=-(h-h_\infty)/\tau_2, \tag{3}$$
$$g_{Cl^-}=\bar{g}_{Cl^-} \quad \frac{dn}{dt}=-(n-n_\infty)/\tau_3.$$

The functions m, h, and n were interpreted as probabilities. Their steady state values, m_∞, h_∞, and n_∞, are strongly potential dependent.

The concentration gradients across the membrane are maintained by ion pumps. These are proteins which pump K^+ ions into the axon and Na^+ and Cl^- ions in the opposite direction. These ion pumps maintain weakly temperature dependent chemical potentials. These pumps act with slow time constants. They are responsible for the second, slow part of the Na^+ and K^+ cycles. The fast responses in the first part of these cycles are due to the opening and closing of respective ion gates. These gates are proteins which open and close in response to variations in the potential difference, V. When open, they allow free flow of the respective ions though a channel in the membrane. Although the flow may be two-way, the concentration gradients insure that Na^+ flows into the axon and K^+ flows out of the axon to reduce these gradients. These processes occur on faster time scales than the pump processes.

II. THE MODIFIED HODGKIN-HUXLEY MODEL

In order to mimic the action potential, or ''spike'' trains experimentally observed in electroreceptor cells from both sharks (dog fish)[3] and catfish,[4] and from the facial cold receptors of the rat,[5] Braun and colleagues have modified the Hodgkin–Huxley equations in order to account for a common feature of the aforementioned cells. The dynamical behavior of these cells is characterized by a subthreshold oscillator or pacemaker.[3,4] Moreover, the oscillation frequency and the temporal patterns of the spikes, including bursting and multimodality of their interspike interval histograms, are strongly temperature dependent. These features were described by Braun *et al.*[6–8] in the modified model by including an additional pair of Na^+ and K^+ channels with slow characteristic response times while ignoring the Cl^- channel. In the notation used by Braun *et al.*, the model is given by $C_M dV/dt=I_1-I_d-I_r-I_{sd}-I_{sr}$, where I_d and I_r are the fast depolarizing and repolarizing (Na^+ and K^+) currents, respectively, and I_{sd} and I_{sr} represent the slow currents which activate at lower membrane potentials. The slow currents account for the oscillatory behavior of this class of neurons. They also account for the fact that this class of neuron model is chaotic for certain parameter values, in this case over certain temperature ranges. The presence of unstable periodic orbits, a signature of chaotic dynamics, has been detected in various sensory neurons, all of which are characterized by oscillators.[4,5,9] A detailed description of the modified Hodgkin–Huxley model, including the numerical values of all parameters as well as their temperature dependencies, has been given[8] and will be summarized below. The model we use here, however, contains no noise, though it is otherwise identical to that of Ref. 8. Thus all the variability we observe here arises from deterministic chaos, and the unstable periodic orbits are observed cleanly. In contrast, the unstable periodic orbits observed in experiments on biological sensory neurons are always obscured by the noise inherent in those neurons and must be detected by statistical methods.[9]

TABLE I. Parameter values for use with the modified Hodgkin–Huxley equations. These include chemical potential μ (mV), time decay τ (ms), conductance g (μS), parameters S (mV^{-1}) (an effective temperature), and $\bar{\mu}$ (mV) (an effective chemical potential) which define equilibrium probabilities through $(1+\exp(-S(V-\bar{\mu})))^{-1}$, and other assorted parameters.

y	Variable	μ	τ	g	S	$\bar{\mu}$
1	$V\sim Na_g$	50		1.5	0.25	−25
2	K_g	−90	2	2.0	0.25	−25
3	Na_p	50	10	0.25	0.09	−40
4	K_p	−90	20	0.40		
	Cl_p	−60		0.1		

$\rho=1.3^{(T-T_0)/10}$ $\eta=0.012$
$\phi=3.0^{(T-T_0)/10}$ $k=0.17$
$T_0=25$ $C_M=1\mu F$

The Hodgkin–Huxley equations were modified by expressing both the Na^+ and K^+ currents as sums of two terms; a fast term describing ion channels relating to spike activity and a slow term describing ion channels relating to the oscillatory activity,[6–8]

$$I_{Na^+}=I_{Na-g}+I_{Na-p},$$
$$I_{K^+}=I_{K-g}+I_{K-p}. \tag{4}$$

The fast currents obey the following equations:

$$I_{Na-g}=\rho\bar{g}_{Na-g}m_{d\infty}(V-\mu_{Na^+}),$$
$$I_{K-g}=\rho\bar{g}_{K-g}n_{K-g}(V-\mu_{K^+}). \tag{5}$$

The slow currents are assumed to satisfy

$$I_{Na-p}=\rho\bar{g}_{Na-p}m_{Na-p}(V-\mu_{Na^+}),$$
$$I_{K-p}=\rho\bar{g}_{K-p}n_{K-p}(V-\mu_{K^+}). \tag{6}$$

The probabilities n_{K-g}, m_{Na-p}, and n_{K-p} are assumed to satisfy the following relaxation equations;

$$\frac{d}{dt}n_{K-g}=-\phi(n_{K-g}-n_{K-g\infty})/\tau_{K-g},$$
$$\frac{d}{dt}m_{Na-p}=-\phi(m_{Na-p}-m_{Na-p\infty})/\tau_{Na-p}, \tag{7}$$
$$\frac{d}{dt}n_{K-p}=-\phi(\eta I_{Na-p}+kn_{K-p})/\tau_{K-p},$$

where the temperature dependent scale factors are $\rho=1.3^{(T-To)/10}$ and $\phi=3.0^{(T-To)/10}$ with $T_0=25\,^\circ$C. These

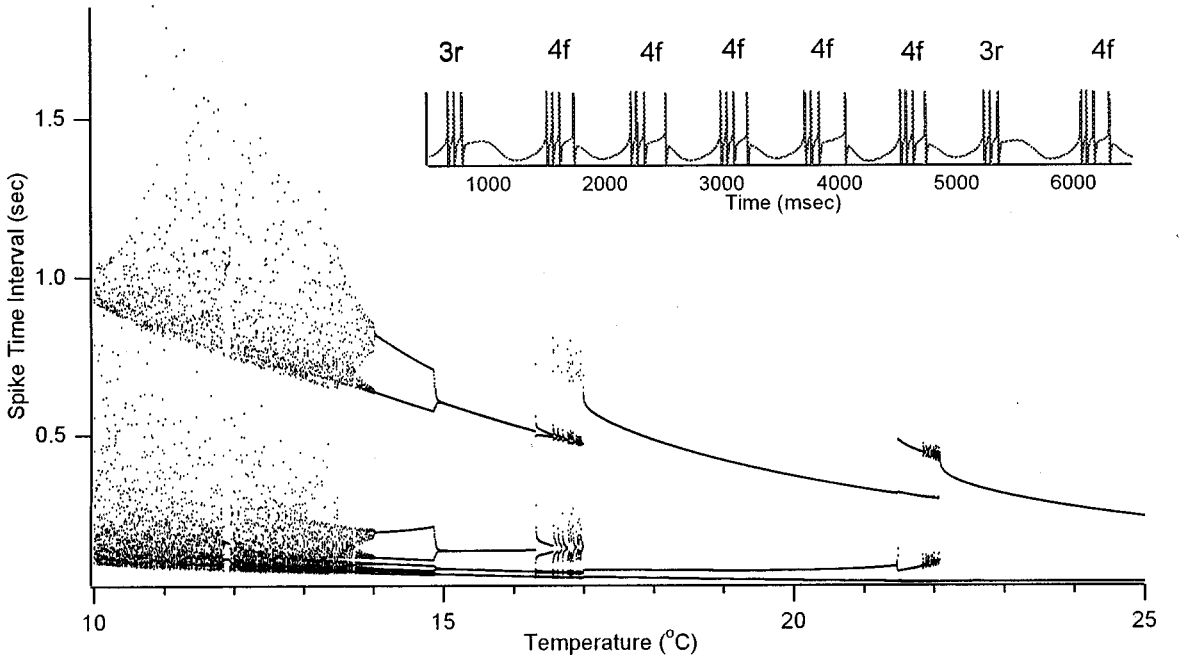

FIG. 1. Bifurcation diagram for the modified Hodgkin–Huxley equations. The time intervals between spikes of $V(t)$ are plotted as a function of temperature T. The diagram shows an alternation between periodic and chaotic behavior. The average number of spikes per burst decreases as the temperature increases. (Inset) Spike train, in which each burst is labeled by a symbol nr, nf.

particular scalings represent the temperature dependencies of the channel conductivities and were introduced in order to account for bifurcations between different types of spike patterns observed in the physiological experiments using temperature as the bifurcation parameter. See Ref. 8 for details. The equilibrium values for all terms which appear in the dynamical system Eqs. (1), (7) and the constitutive Eqs. (4)–(6) are summarized in Table I. Assuming homogeneity along the axon, $I=0$ in (1) and the Eqs. (1) and (7) reduce to four ordinary differential equations for $(V,n_{K-g},m_{Na-p},n_{K-p})=(y_1,y_2,y_3,y_4)$.

III. RESULTS: THE TOPOLOGY OF BURSTING

These modified Hodgkin–Huxley equations have been studied by numerical integration. We have used a standard RK4 procedure[10] with a constant step size of $dt=0.05$ ms. Integrations were carried out for the parameter values shown in Table I, for temperatures in the range $T=10$–25 °C.

In this temperature range the potential $V(t)$ exhibits a series of peaks (''spike burst'') followed by a return to a polarized state ($V\sim-65$ mV). The burst consists of one to six depolarization peaks, all sharp and of approximately the same height. The interspike interval increases monotonically between peaks in a single burst. The last spike in a burst of n spikes is usually followed by a monotonic return to the repolarization minimum (nf), although it is sometimes followed by an incomplete depolarization rise, observed as a broad maximum well below the typical sharp spike height, and then a return to the repolarization minimum (nr). Bursting is a common behavior observed in a wide variety of neurons. As the temperature ranges from $T=10$–25 °C, the average number of spikes per burst decreases from six to one. In Fig. 1 we record the time intervals between successive spikes of $V(t)$ vs T as the temperature is slowly scanned from $T=10$–25 °C. Within some chaotic regions we can clearly see periodic windows followed by period doubling cascades into chaos. In the inset to Fig. 1 we show a series of spike train bursts, all of which are labeled by symbols nf, nr. The notation will be explained below.

In order to study the type of chaos[11] characteristic of this model, we generated strange attractors by integrating the equations at many values of T for which chaos was observed. The strange attractors were then projected into the six planes which are formed from pairs of the four variables y_1, y_2, y_3, y_4. In all cases the projection into the y_1–y_2 plane was a slightly deformed circle. This means that y_1 and y_2 are in quadrature, with y_2 following y_1 by $\sim\pi/2$ radians. As a result, the modified Hodgkin–Huxley equations for these parameter values describe a system which is effectively three dimensional. This means that the topological methods developed to classify low (3) dimensional dynamical systems[11,12] can be applied to these equations.

The topological analysis procedure involves several steps:

(1) The strange attractor is embedded in a three-dimensional phase space.
(2) Unstable periodic orbits of low period are located by the method of close returns.
(3) The topological invariants of these orbits, their linking numbers and relative rotation rates,[13] are computed.
(4) A knot holder or template is determined from these topological invariants. The knot holder accounts for the organization of all the unstable periodic orbits in the strange attractor.
(5) Finally, the validity of this template is tested by predict-

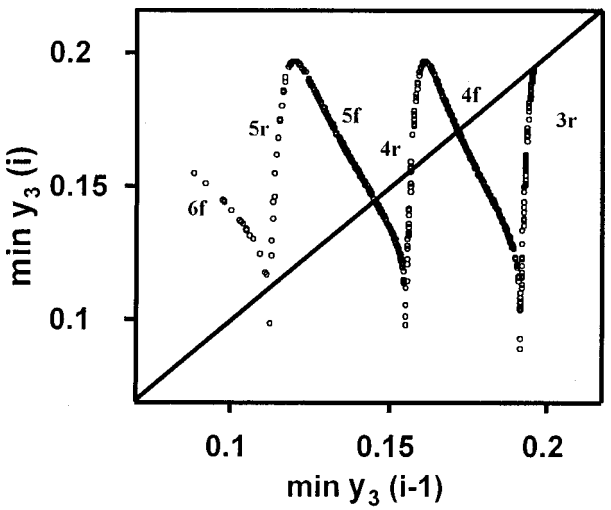

FIG. 2. First return map for the modified Hodgkin–Huxely equations for $T=12$ °C. The Poincaré section is defined by the minima of y_3 during the repolarization stage. Local torsion increases systematically from branch to branch, as shown by the branch labels.

ing the linking numbers of additional periodic orbits, and comparing these predictions against additional orbits found in the attractor.

We studied the attractors of the modified Hodgkin–Huxley model in three different embeddings. These were the phase spaces (x_1,x_2,x_3) with the identifications $(x_1=y_3,x_2=y_4,x_3=y_1)$ and the differential $(x_1=y_3,x_2=\dot{x}_1,x_3=\dot{x}_2)$ and integral $(x_1,x_2=\dot{x}_1=y_3,x_3=\dot{x}_2)$ embeddings. In the latter two embeddings the three variables are differentially related to each other, $x_3=\dot{x}_2=\ddot{x}_1$. The latter two embeddings are useful because linking numbers are particularly easy to compute in these embeddings.[11,12] We will describe our analysis for the differential embeddings based on the variable y_3. Identical results were found for all three embeddings.

Each strange attractor has a ''hole'' in the middle. This enabled us to construct a global Poincaré section. This section was chosen at the repolarization minimum. Specifically, we chose $dy_3/dt=0, y_3<$ some threshold, to define the global Poincaré section. The threshold was chosen to distinguish between the minimum values of y_3 during the repolarizaiton stage and the minimum values of y_3 between spikes in a burst. A return map on this Poincaré section is shown in Fig. 2 for $T=12$ °C. This return map shows that

(1) The modified Hodgkin-Huxley equations are highly dissipative.
(2) It is possible to locate many distinct period one orbits in some strange attractors.
(3) The period one orbits are organized in a very specific way with respect to each other.
(4) Branches labeled nf describe bursts with n spikes. Branches labeled nr describe bursts with n spikes and an extra incomplete spike.
(5) The period one orbits nf are orientation reversing (flip saddles) while the period one orbits nr are orientation preserving (regular saddles).
(6) The orientation reversing orbits nf are less unstable than the orientation preserving orbits nr.

By following perturbations around the period one orbits, we determined that the local torsion about nr is $\pi\times 2n$ radians while the local torsion about nf is $\pi\times(2n-1)$ radians. Thus, the local torsion increases systematically from branch to branch in the return map of Fig. 2.

This information is sufficient to reveal that the template which describes the strange attractors generated by the modified Hodgkin-Huxley equations is a spiral template, also called a ''gateau roulé'' or ''jelly-roll.'' There are two such templates; one rolls up ''from outside to inside,'' while the other rolls up ''from inside to outside.'' These are shown in

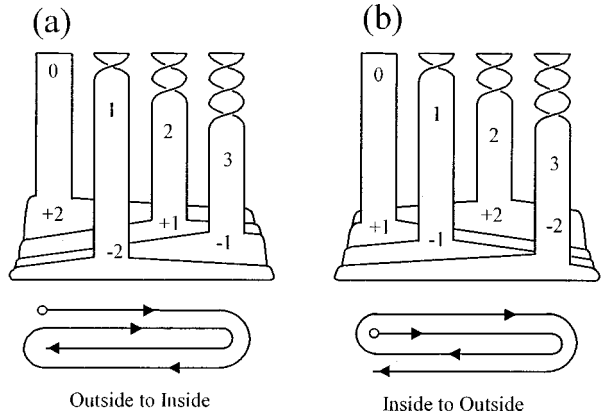

FIG. 3. Scroll template rolling up (a) from outside to inside, (b) from inside to outside.

TABLE II. Template matrix and array for scroll template; outside to inside.

Branch	Array	0	1	2	3	4	5	6	7	8	9
0	$+N-0$	0	0	0	0	0	0	0	0	0	0
1	$-N+0$	0	1	2	2	2	2	2	2	2	2
2	$+N-1$	0	2	2	2	2	2	2	2	2	2
3	$-N+1$	0	2	2	3	4	4	4	4	4	4
4	$+N-2$	0	2	2	4	4	4	4	4	4	4
5	$-N+2$	0	2	2	4	4	5	6	6	6	6
6	$+N-3$	0	2	2	4	4	6	6	6	6	6
7	$-N+3$	0	2	2	4	4	6	6	7	8	8
8	$+N-4$	0	2	2	4	4	6	6	8	8	8
9	$-N+4$	0	2	2	4	4	6	6	8	8	9

TABLE III. Template matrix and array for scroll template; inside to outside.

Branch	Array	0	1	2	3	4	5	6	7	8	9
0	0	0	0	2	2	4	4	6	6	8	8
1	-1	0	1	2	2	4	4	6	6	8	8
2	$+1$	2	2	2	2	4	4	6	6	8	8
3	-2	2	2	2	3	4	4	6	6	8	8
4	$+2$	4	4	4	4	4	4	6	6	8	8
5	-3	4	4	4	4	4	5	6	6	8	8
6	$+3$	6	6	6	6	6	6	6	6	8	8
7	-4	6	6	6	6	6	6	6	7	8	8
8	$+4$	8	8	8	8	8	8	8	8	8	8
9	-5	8	8	8	8	8	8	8	8	8	9

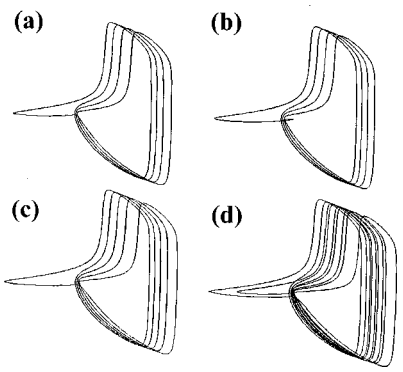

FIG. 4. Three period one orbits (a) $4f$; (b) $4r$; (c) $5f$; and one period two orbit (d) $(4f,5f)$ extracted from the strange attractor at $T=12$ °C.

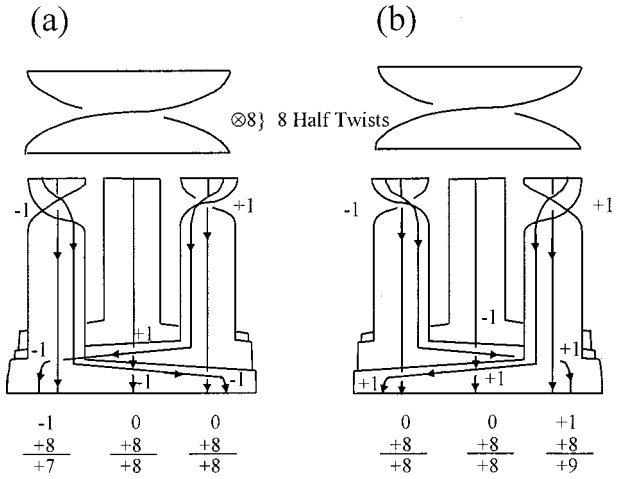

FIG. 5. Computation of the linking numbers of the period two orbit $(4f,5f)$ with the period one orbits $4f,5r,5f$ on the two scroll templates. The ''outside to inside'' scroll template (a) is compatible with the Hodgkin–Huxley strange attractor of the modified Hodgkin–Huxley equations.

Fig. 3. One of these, the one which rolls up ''from outside to inside,'' has been identified in the Duffing oscillator[14] and has been observed in experiments performed on a YAG laser.[15]

We provide the algebraic descriptions for these two templates in Tables II and III. In these tables, the branches are labeled by integers 0,1,2,... which describe the local torsion of the period one orbits in these branches, $T(i,i)=i$. The off-diagonal matrix elements are twice the linking numbers of the period one orbits in the two branches, $T(i,j)=2L(i,j)$. The array information identifies the order in which the branches are joined at the bottom; smaller integers identify closer branches.

For both templates, adjacent branches with local torsion $2n,2n+1$ form a (direct) smale horseshoe with global torsion n, and those with local torsion $2n+1,2n+2$ form a reverse smale horseshoe with global torsion n.[11,13,14] It is not possible to distinguish between the two types of scroll templates by studying strange attractors confined to only two adjacent branches of a scroll template. The distinction can only be made by studying strange attractors which extend over three or more branches.

Accordingly, we located period one orbits $4f$, $4r$, and $5f$ and the period two orbit $(4f,5f)$ in the strange attractor for $T=12$ °C. They were located using the first and second return maps on the Poincaré section. These orbits are shown in Fig. 4, in the differential embedding. The linking numbers for these orbits are

$$\begin{aligned} &L(4f;4r)=4, \quad L(4f;(4f,5f))=7,\\ &L(4f;5f)=4, \quad L(4r;(4f,5f))=8,\\ &L(4r;5f)=4, \quad L(5f;(4f,5f))=8. \end{aligned} \tag{8}$$

These linking numbers are consistent with the outside to inside scroll template[13] and rule out the other scroll template. The linking numbers for the period two orbit in the ''inside to outside'' scroll are $L(4f;(4f,5f))=8, L(4r;(4f,5f))=8$, and $L(5f;(4f,5f))=9$.

In Fig. 5 we illustrate how the linking numbers are computed on the two templates. The three branches on which the three period one orbits $4f$, $4r$, and $5f$ live are shown. Each period one orbit is represented by a vertical line in the corresponding branch. The period two orbit $(4f,5f)$ is shown propagating through the two outer branches. Each time the period two orbit crosses a period one orbit, an integer ± 1 is assigned. The integer is $+1$ if the crossing is right handed, -1 if left handed. The handedness is determined by the standard convention. Rotate the tangent vector to the flow on the upper filament into the tangent vector to the flow on the lower filament through the smaller angle. The rotation is either right handed or left handed, as per the usual convention. The period two orbit crosses a period one orbit a number of times. Two crossings are shown explicitly, along with the signs for each of the crossings. The template for these three branches has eight additional half-twists, in which the period two orbit crosses each of the period one orbits $+16$ times. The linking number is half the signed number of crossings. Specifically, it is 8 plus half the sum of the two crossings shown explicitly for each of the period one orbits. In the template shown in Fig. 5(a) the linking numbers are 7, 8, and 8 for the three orbits with local torsions 7, 8, and 9. These integers are compatible with those computed from the unstable periodic orbits extracted from the strange attractor. In the template shown in Fig. 5(b) (''inside to outside'') the linking numbers for the corresponding period one orbits are 8, 8, and 9. These integers are incompatible with the data.

IV. DISCUSSION, CONCLUSION, AND SUMMARY

Apart from simple firings at irregular time intervals and oscillatory behavior, *bursting* is the most common pattern of action potential sequences observed in a wide variety of neurons. Bursts are frequently composed of two to several action potentials occurring with sequentially increasing interspike time intervals. We emphasize that this behavior is so frequently encountered as to be generic to several classes of neurons. It is well described by the Hodgkin–Huxley model modified to include the slow oscillator as used here. We show that the bursts are indeed the result of a chaotic dynamics and that the characteristic firing patterns arise directly from the topology of the chaotic attractor. Thus, in the view presented here, the very familiar burst pattern of sensory

neurons is fundamentally a topological object. It is remarkable that only a small number (about four, plus variants) of different topologies are sufficient to describe a wide range of chaotic systems observed in physical systems.[11] Chaos in the present model resides in the same class as that of the YAG laser.

The Hodgkin–Huxley equations have been modified to describe neural spike train data observed in three different temperature dependent neurons with oscillators. As the temperature is gradually increased from 10 to 25 °C the number of spikes per burst decreases from 6 to 1, with an alternation between periodic and chaotic behavior. In chaotic regions, there is an unpredictabe alternation between bursts with n spikes per burst and those with $n \pm 1$ spikes per burst. We have shown that in the chaotic regime the strange attractors are effectively three dimensional. We have constructed a number of three-dimensional embeddings and studied strange attractors in each. The results are independent of the embedding used. It is always possible to construct a global Poincaré section. The first return map on the Poincaré section reveals that the dynamics is highly dissipative. Further, the distinct branches of the return map are organized in a very specific way. That is, the local torsion of the period one orbit in a branch increases systematically between adjacent branches. As a result the template, which provides a caricature for the dynamics, and which also classifies the type of stretching and squeezing mechanisms which generate the strange attractor and organize all the unstable periodic orbits in it in a unique way, is a scroll. We have extracted unstable period one and period two orbits from the strange attractor and computed their linking numbers to identify the scroll mechanism. The scroll winds up from outside to inside. Such scrolls have previously been identified in the Duffing attractor[14] and have been observed in the YAG laser.[15]

As the temperature is increased, the first return map, shown in Fig. 2, moves to the left. When the map reaches tangency with the diagonal, a saddle node bifurcation occurs, a stable period one orbit is created on a template branch not previously occupied, and periodic behavior is observed. As the temperature increases further, the stable period one orbit loses its stability in the usual way, and a new strange attractor develops. This systematic behavior has also previously been observed in the Duffing attractor[14] and the YAG laser.[15]

ACKNOWLEDGMENTS

This work is supported in part by the Office of Naval Research, Physical Sciences Division, and by the Department of Energy.

[1] A. L. Hodgkin, A. F. Huxley, and B. Katz, Arch. Sci. Phys. Nat. **3**, 129 (1949); J. Physiol. (London) **116**, 424 (1952); A. L. Hodgkin and B. Katz, *ibid.* **109**, 240 (1949); A. L. Hodgkin and A. F. Huxley, *ibid.* **116**, 449 (1952); **116**, 473 (1952); **116**, 497 (1952); A. L. Hodgkin, Biol. Rev. Cambridge Philos. Soc. **26**, 339 (1952).
[2] A. L. Hodgkin and A. F. Huxley, J. Physiol. (London) **117**, 500 (1952).
[3] H. A. Braun, H. Wissing, K. Schäfer, and M. C. Hirsch, Nature (London) **367**, 270 (1994).
[4] K. Schäfer, H. A. Braun, R. C. Peters, and F. Bretschneider, Pflugers Arch. Ges. Physiol. Menschen Tiere **429**, 378 (1995); H. A. Braun, K. Schäfer, K. Voigt, R. Peters, F. Bretschneider, X. Pei, L. Wilkens, and F. Moss, J. Comp. Neurol. **4**, 335 (1997).
[5] H. A. Braun, M. Dewald, K. Schäfer, K. Voigt, X. Pei, and F. Moss, J. Comp. Neurosci. **7**, 17 (1999).
[6] H. A. Braun, M. T. Huber, M. Dewald, and K. Voigt, in *Applied Nonlinear Dynamics and Stochastic Systems Near the Millenium*, edited by J. B. Kadtke and A. Bulsara (American Institute of Physics, New York, 1997), p. 281.
[7] F. Moss, X. Pei, K. Dolan, H. A. Braun, M. Huber, and M. Dewald, in *Proceedings of the Italian Summer School on Biophysics*, edited by S. Chillemi and M. Barbi (World Scientific, Singapore, 1998), p. 60.
[8] H. A. Braun, M. T. Huber, M. Dewald, K. Schäfer, and K. Voigt, Int. J. Bifurcation Chaos Appl. Sci. Eng. **8**, 881 (1998).
[9] X. Pei and F. Moss, Nature (London) **379**, 618 (1996); X. Pei, K. Dolan, F. Moss, and Y.-C. Lai, Chaos **8**, 853 (1998).
[10] W. H. Press, S. A. Teukolsky, B. R. Flannery, and W. T. Vetterling, *Numerical Recipes* (Cambridge: University Press, Cambridge, 1986).
[11] R. Gilmore, Rev. Mod. Phys. **70**, 1455 (1998).
[12] G. B. Mindlin, H. G. Solari, M. A. Natiello, R. Gilmore, and X.-J. Hou, J. Nonlinear Sci. **1**, 147 (1991).
[13] H. G. Solari and R. Gilmore, Phys. Rev. A **37**, 3096 (1988).
[14] R. Gilmore and J. W. L. McCallum, Phys. Rev. E **51**, 935 (1995).
[15] G. Boulant, M. Lefranc, S. Bielawski, and D. Derozier, Phys. Rev. E **55**, 5082 (1997).